

Supporting Information

Transmissive-to-black fast electrochromic switching from long conjugated pendant group and highly dispersed polymer/SWNT

Qiang Zhang,^a Chou-Yi Tsai,^a Taufik Abidin,^a Jyh-Chiang Jiang,^a Wan-Ru Shie,^a Lain-Jong Li^b and Der-Jang Liaw^{*a}

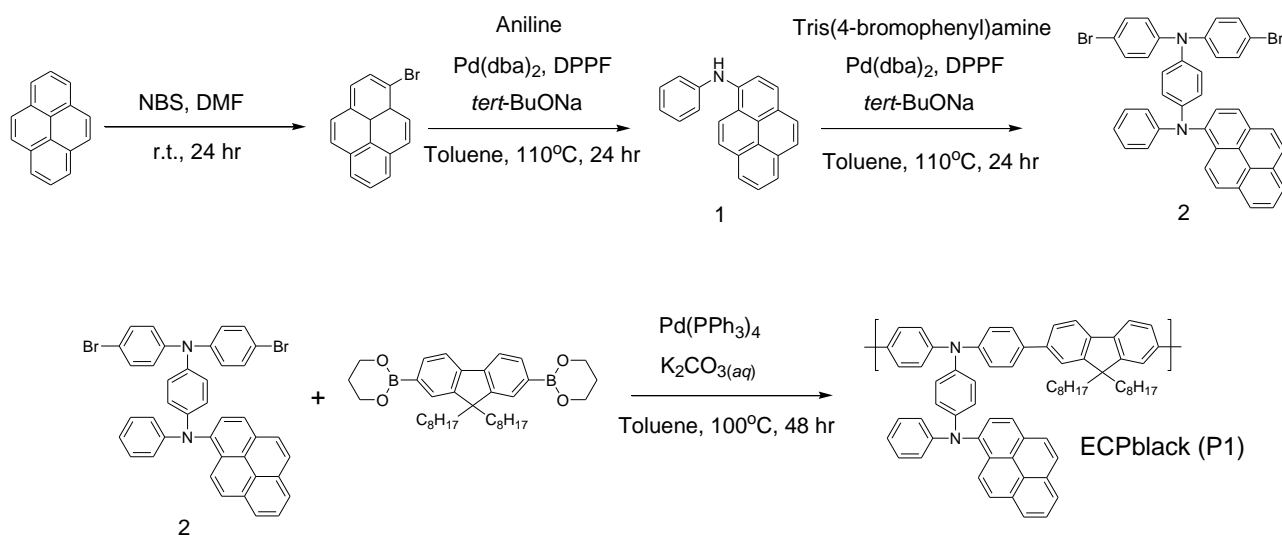
^a Department of Chemical Engineering, National Taiwan University of Science and Technology, 10607 Taipei, Taiwan

^b Material Science and Engineering, King Abdullah University of Science and Technology

Materials

Pyrene, triphenylamine, *N*-bromosuccinimide (NBS), aniline, *p*-anisidine, 4-dodecylaniline, 1-bromo-4-iodobenzene, bis(dibenzylideneacetone)palladium(0) (Pd(dba)₂), 1'1'-bis(diphenylphosphino)ferrocene (DPPF), sodium *tert*-butoxide, 9,9-dioctylfluorene-2,7-diboronic acid bis(1,3-propanediol) ester, tetrakis(triphenylphosphine)palladium(0) (Pd(PPh₃)₄), potassium carbonate (K₂CO₃), *n*-butyllithium solution (2.5M), 2-Isopropoxy-4,4,5,5-tetramethyl-1,3,2-dioxaborolane and tetrabutylammonium perchlorate (TBAP) were purchased from Aldrich. 9,9-Dioctylfluorene-2,7-diboronic acid bis(1,3-propanediol) ester was used after recrystallization from hexane. Aniline, *p*-anisidine and 4-dodecylaniline were distilled under nitrogen before use. The other chemicals were used without purification. The solvents (analytical grade) were purchased from Merck. Tetrahydrofuran (THF) and toluene were distilled from sodium/benzophenone (deep purple) under nitrogen before use. Dimethylformamide (DMF) and acetonitrile (CH₃CN) were distilled from calcium hydride (stirring for 12 hours) under nitrogen before use. All other reagents were used as received. CoMoCAT single walled carbon nanotube (SWNT) was purchased from West Technology Limited.

Syntheses of monomers and polymers



Scheme S1. Synthetic route of monomers **1**, **2** and polymer **ECPblack (P1)**

1-Bromopyrene¹ and tri(4-bromophenyl)amine² were synthesized according to the literatures.

N-phenylpyren-1-amine (**1**, Figure S1)

1-Bromopyrene (12.5 g, 44 mmol), aniline (8.9 g, 89 mmol), DPPF (490 mg, 0.9 mmol), Pd(dba)₂ (500 mg, 0.9 mmol), sodium *tert*-butoxide (6.4 g, 67 mmol), and toluene (100 mL) were placed in a 500 mL three-neck round-bottom flask equipped with a condenser. The mixture was heated and stirred at 110 °C for 24 h under nitrogen flow. After reaction, the reaction mixture was distilled at 55 °C under reduced pressure (50 torr). Residual aniline was removed by distilling under nitrogen flow at 110 °C with reduced pressure (0.1 torr). The crude product was washed by methanol then purified by silica gel column chromatography (*n*-hexane : dichloromethane (DCM) = 1 : 2) which was dried under reduced pressure then recrystallized with methanol to afford 4.56 g pure product (yield: 35%, mp = 156°C). ¹H NMR (600 MHz, CDCl₃): δ_H (ppm): 5.40-6.75 (1H,

H₁₅); 6.98-7.04 (1H, H₁₉); 7.05-7.12 (2H, H₁₇); 7.30-7.36 (2H, H₁₈); 7.93-7.95 (1H, H₁₃); 7.95-7.97 (1H, H₁₂); 7.97-8.00 (1H, H₇); 8.00-8.02 (1H, H₆); 8.02-8.05 (1H, H₅); 8.08-8.11 (2H, H₃ and H₉), 8.15-8.18 (2H, H₉ and H₁₀). ¹³C NMR (150 MHz, CDCl₃), δ_c (ppm): 116.96 (C₁₇), 118.99(C₁₃), 118.99(C₁₂), 120.61 (C₁₉), 121.20 (C₂), 121.20 (C₁₀), 123.19(C₁₄), 124.37 (C₂₁), 124.72 (C₉), 125.09(C₁), 125.50 (C₃), 125.90 (C₁₁), 126.02(C₅), 126.98 (C₆), 127.31(C₄), 129.40 (C₁₈), 131.30 (C₄), 131.64 (C₈), 136.50 (C₂₀), 144.80 (C₁₆). IR (KBr): 3400 cm⁻¹(NH stretch); 3000 cm⁻¹ & 2900 cm⁻¹ (ArH); 1495 cm⁻¹ (NH bend); 1600 cm⁻¹ and 1475 cm⁻¹ (CC aromatic stretch); 1300 cm⁻¹ (CN stretch); 800 cm⁻¹ (NH out of plane bending); 690 cm⁻¹& 750 cm⁻¹ (monosubstitute out of plane bending). Anal. calcd for C₂₂H₁₅N: C 90.07%, H 5.15%, N 4.77%; found: C 91.04%, H 5.09%, N 5.17%. HRMS (ESI) *m/z*: [M] calcd for C₂₂H₁₅N, 293.12; found, 293.1199.

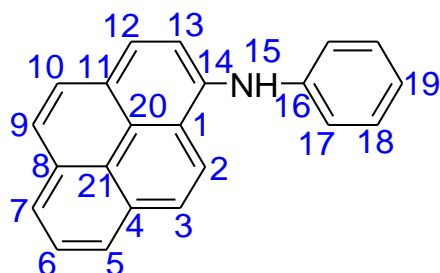


Figure S1. Structure of monomer 1.

***N,N*-Bis(4-bromophenyl)-*N'*-phenyl-*N'*-(pyrene-1-yl)-1,4-phenylenediamine (2, Figure S2)**

Tris(4-bromophenyl)amine (6.7 g, 14 mmol), compound 1 (3.6 g, 9 mmol), Pd(dba)₂ (115 mg, 0.2 mmol), DPPF (110 mg, 0.2 mmol), sodium *tert*-butoxide (1.78 g, 18.54 mmol) and toluene (70 mL) were charged in a 250 mL three-necked flask equipped with a condenser and kept under nitrogen flow. The mixture was heated to reflux for 24 h. After the completion of the reaction, the solvent was removed under vacuum and the residue was extracted with DCM and dried, and the residue was purified by silica gel column chromatography (*n*-hexane : DCM = 1 : 2). Then the product was recrystallized from a solvent mixture (*n*-hexane : DCM = 2 : 1), and 3.86 g of light yellow-green solid was obtained (yield: 60%). ¹H NMR (600 MHz, CDCl₃): δ_H (ppm)= 6.89-6.94 (2H, H₁₆); 6.94-6.97 (4H, H₂₆); 6.97-7.10 (2H, H₂₂); 6.97-7.04 (2H, H₂₃); 7.04-7.10 (1H, H₁₈); 7.19-7.26 (2H, H₁₇); 7.29-7.37 (4H, H₂₇); 7.96-7.98 (1H, H₁₃); 7.98-8.00 (1H, H₉); 8.00-8.03(1H, H₆); 8.06-8.11 (2H, H₂ and H₃); 8.13-8.16 (1H, H₁₀); 8.16-8.17 (1H, H₅); 8.17-8.19(1H, H₇); 8.17-8.19(1H, H₁₀); 8.19-8.22(1H, H₁₂). ¹³C NMR (150 MHz, CDCl₃), δ_c (ppm): 114.93 (C₂₅), 140.65 (C₂₀), 144.93 (C₁₄), 146.54 (C₁₉), 148.51 (C₂₈), 121.63 (C₁₈), 123.19(C₇ and C₅), 123.26 (C₂₃ and C₂₂), 124.81 (C₁₆ and C₂₆), 125.14(C₁₀), 125.28 (C₁₂), 126.00 (C₂₄), 126.08 (C₂₁), 126.25 (C₆), 126.36 (C₁₁), 127.18 (C₂ and C₃), 127.59 (C₉), 127.94 (C₁₃), 129.18 (C₁₇), 129.67 (C₁), 131.03 (C₄), 131.24 (C₈), 132.23 (C₂₇). IR (KBr) 1020 cm⁻¹ (ArH stretch); 1600 cm⁻¹& 1475 cm⁻¹ (CC aromatic stretch); 1320 cm⁻¹ & 1270 cm⁻¹ (CN stretch); 510 cm⁻¹ (CBr stretch). Melting point (mp) is 223°C. Anal. calcd for C₄₀H₂₆Br₂N₂: C 69.18%, H 3.77%, N 4.03%; found: C 69.50%, H 3.84%, N 4.35%. HRMS (ESI) *m/z*: [M] calcd for C₄₀H₂₆Br₂N₂, 694.04; found, 694.0392.

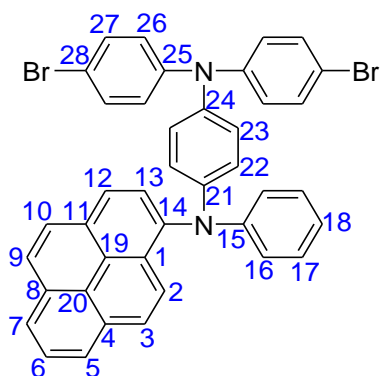


Figure S2. Structure of monomer **2**.

Synthesis of Polymer ECPblack (P1, Figure S3)

To the 250 mL three-necked flask was added monomer **2** (386 mg, 0.93 mmol) with 9,9-dioctylfluorene-2,7-diboronic acid bis(1,3-propanediol) ester (519 mg, 0.93 mmol) for **ECPblack (P1)**. The flask equipped with a condenser was evacuated and filled with nitrogen several times to remove traces of air, then the degassed toluene (5 mL) was added. Once the two monomers were dissolved, tetrakis(triphenylphosphine)palladium(0) (Pd(PPh₃)₄) (3 mg, 0.026 mmol) and potassium carbonate aqueous solution (10 ml, 3 M) was added and the mixture was stirred for 48 hrs at 100 °C under nitrogen flow. The reaction mixture was cooled to room temperature and the organic layer was separated, washed with water and precipitated into methanol. The green polymer sample was filtered and washed with excess methanol, then dried and purified by a Soxhlet extraction with acetone for 2 days, after which 729 mg (yield: 85%) of polymer was obtained. ¹H NMR (600 MHz, C₆D₅Cl): δ_H (ppm)= 0.76-0.80 (3H, H₄₃); 0.87-0.90 (2H, H₃₇); 0.90-0.95(2H, H₄₀); 0.95- 1.01(2H, H₃₈); 1.01-1.04 (m, 2H, H₄₁); 1.04-1.10 (2H, H₃₉); 1.10-1.15 (2H, H₄₂); 2.10-2.25 (2H, H₃₆); 6.86-6.91 (1H, H₁₈); 6.91-6.93 (2H, H₂₃); 6.93-6.95 (1H, H₁₃); 6.95-6.97 (2H, H₁₇); 6.97-7.20(2H, H₁₆); 7.12-7.15 (2H, H₂₂); 7.15-7.19 (1H, H₁₂); 7.25-7.32 (4H, H₂₆); 7.58-7.63 (1H, H₅); 7.63-7.68 (4H, H₂₇) 7.74-7.78 (1H, H₇); 7.78-7.81 (1H, H₆); 7.81-7.84 (1H, H₁₀); 7.84-7.88 (2H, H₃₀); 7.88-7.90(1H, H₂); 7.90-7.94 (1H, H₃); 7.98-8.00 (2H, H₆); 8.00-8.03 (1H, H₉); 8.31-8.35 (1H, H₇). ¹³C NMR (150 MHz, C₆D₅Cl), δ_C (ppm): 138.16 (C₂₅), 142.26 (C₂₉), 142.48 (C₃₂), 143.32 (C₂₀), 149.55 (C₂₈), 151.40 (C₁₉), 154.40(C₃₃), 121.34(C₁₃), 122.73 (C₇), 123.46(C₁₀), 124.04 (C₁₈), 124.09(C₁₂), 125.60 (C₁₇), 126.04 (C₅), 126.44 (C₂₆), 127.65(C₃), 127.75 (C₉), 128.09 (C₃₁), 128.25 (C₆), 128.54 (C₂₇), 128.67 (C₁₁), 129.03 (C₁), 129.70 (C₂) 130.07 (C₃₀), 130.38 (C₁₅), 130.71(C₅), 131.71 (C₁₆), 131.83 (C₂₃), 132.16 (C₂₂), 133.64 (C₈), 133.81 (C₄), 136.48 (C₂₄), 138.16 (C₂₅), 16.53 (C₄₃) 25.16 (C₄₂), 26.63 (C₃₇), 31.79(C₄₀), 32.41 (C₃₉), 32.71 (C₄₁), 34.31 (C₃₈), 43.13(C₃₆), 57.88 (C₃₅). IR (KBr) 3050 cm⁻¹ (sp² C-H stretch); 2930 cm⁻¹ & 2850 cm⁻¹ (sp³ C-H stretch); 1600 cm⁻¹ & 1475 cm⁻¹ (C=C aromatic stretch) 1500 cm⁻¹ (C-H of CH₂ bending) 1450 cm⁻¹ (C-H of CH₃ bending) 1260 cm⁻¹ (C-N stretch); 750 cm⁻¹ (Long alkane chain bend). Anal. calcd for (C₇₁H₇₂N₂)_n: C 89.76%, H 7.21%, N 3.03%; found: C 89.26%, H 7.06%, N 2.96%.

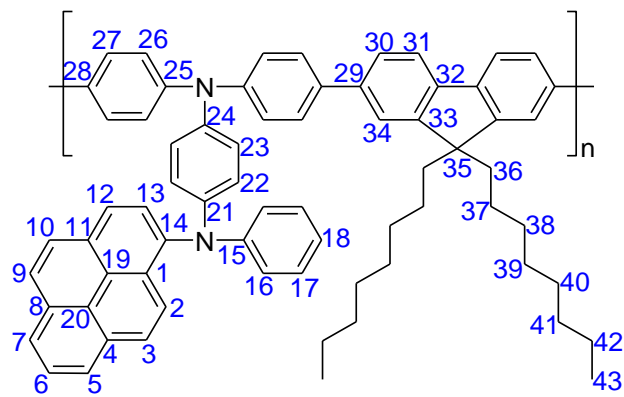


Figure S3. Structure of polymer **ECPblack (P1)**

Molecules Weight Characterization and Solubility

GPC measurements were conducted to measure the molecular weight and polydispersity complex relative to the polystyrene standards. The results are summarized in Table S1. **ECPblack** has a number average molecular weight (M_n) of 2.08×10^4 g/mol and a weight average molecular weight (M_w) of 2.93×10^4 g/mol. **ECPblack** was highly soluble in DCM, toluene, chlorobenzene (CB), xylene, and benzene because it possessed the noncoplanar structure of triarylamine and fluorene, asymmetric structure of phenyl and pyrene units as well as alkyl chains as pendant groups, resulting in large spaces for solubility enhancement.

Thermal Properties

The rigid structure of triphenylamine can enhance the T_g and thermal stability as studied in the literature.³ The thermal stability of **ECPblack** was determined by thermogravimetric analysis (TGA) and its phase transition behavior was evaluated with differential scanning calorimetry analysis (DSC) techniques. Results are summarized in Table S1. There are no melting endotherms up to the decomposition temperatures on the DSC thermograms. This supports the proposed amorphous nature of this triphenylamine-containing polymer.⁴ The glass transition temperature (T_g), 10% weight-loss temperatures (T_{d10}) in nitrogen and air, and char yield (CR) at 800 °C in nitrogen and air of **ECPblack** were 169 °C, 445 °C and 371 °C, 62% and 3% (Table S1), respectively.

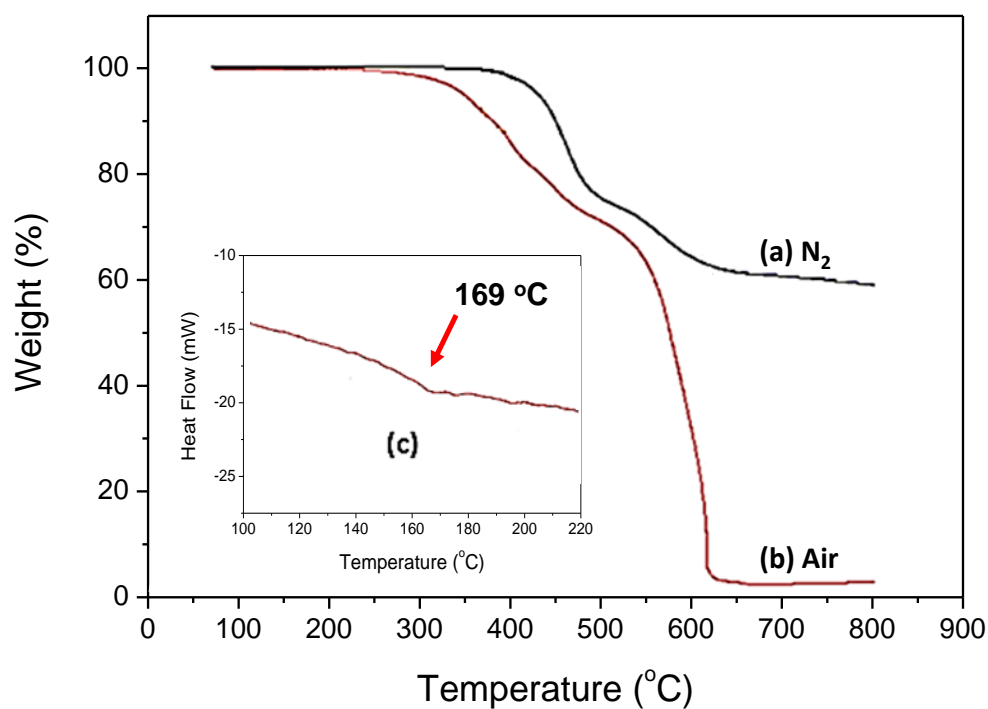


Figure S4. (a) and (b) TGA graphs of ECPblack in nitrogen and air. (c) DSC graph of ECPblack.

Optical properties

The optical properties of **ECPblack** were investigated by UV-vis and photoluminescence (PL) spectroscopy when in solid state and in various solvents (*ca.* 1×10^{-5} M) such as toluene, THF and NMP, as shown in Figure S5. The optical properties were summarized in Table S1. We ascribed the peak at 393 nm to a π - π^* transition derived from the conjugated polymer backbone. The absorption wavelength of **ECPblack** in solid-state film causes a bathochromic shift of the low-energy transition band at 399 nm. This hypsochromic shift may be attributed to the more disordered morphology of the backbone, resulting from conformational fluctuations of the highly twisted and bulky propeller-shaped *bi*-triarylamine moiety.⁵ The optical bandgap was determined from the onset absorption of **ECPblack** in solid film form, with a bandgap of 2.7 eV for **ECPblack**. The normalized fluorescence emission spectra of the conjugated polymer **ECPblack** in various solvents exhibited a strong solvent polarity dependence and are also shown in Figure S5. The fluorescence emission spectra underwent remarkable bathochromic shifts with an increase of the solvent polarity, exhibiting maximum emission peaks at 514, 558, and 595 nm in toluene, THF, and NMP, respectively. The solvatochromism could be attributed to the fast intramolecular charge-transfer process resulting in a large change of dipole moment in the excited state.⁶ Therefore, the higher the polarity of the solvent, the lower the energy of the relaxed state and the larger red-shift of the emission spectrum. The fluorescent quantum yield of **ECPblack** was 45.1% in toluene solution.

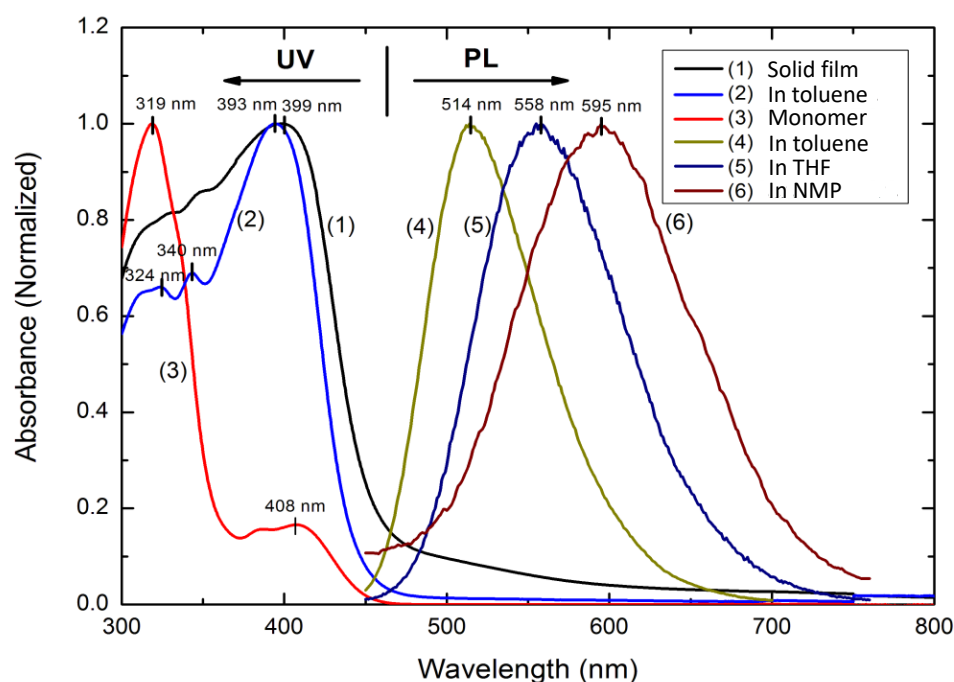


Figure S5. Normalized absorption and PL spectra of **ECPblack**. The absorption of **ECPblack** film (1) and dissolved in toluene (2). The absorption of monomer **2** dissolved in toluene (3). The PL of **ECPblack** were measured when dissolved in toluene (4), THF (5) and NMP (6).

Electrochemical Properties

The electrochemical behavior of **ECPblack** was investigated by cyclic voltammetry (CV). The two reversible redox couples with the two $E_{1/2}$ values of 0.65 V and 0.98 V of conjugated polymer film on ITO-glass, which were in good agreement with the oxidation order of the two nitrogen atoms in the bi-triarylamine groups of **ECPblack**. The CV of **ECPblack**/graphene/PET showed weaker oxidation waves than **ECPblack**/ITO/Glass, due to the higher resistance of the graphene electrode. The two oxidation peaks do not appear in the same bias potential, so the first electron is removed from the HOMO of the molecule and the second electron was removed from the SOMO. From the oxidation potential relative to ferrocene/ferrocenium, which corresponds to -4.8 eV for ferrocene below the vacuum level, the HOMO of the **ECPblack** can be determined by the equation: $\text{HOMO} = -(E_{\text{onset}}^{\text{ox}} - E_{\text{onset}}^{\text{Fc}}) - 4.8$. The LUMO and E_g are found to be -2.3 eV and 2.7 eV, respectively. All the corresponding data are collected in Table S1.

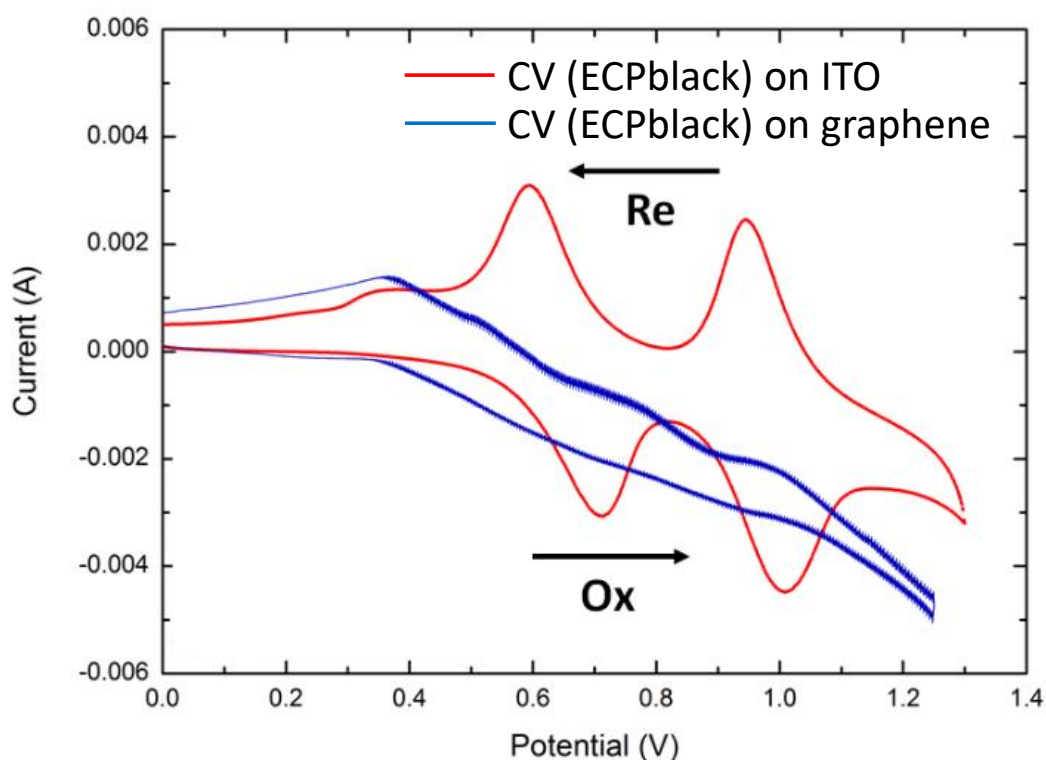


Figure S6. Cyclic voltammograms of the conjugated polymer **ECPblack** film. The CV of **ECPblack** was performed in acetonitrile solutions containing 0.1 M TBAP. ITO-coated glass and graphene-coated PET were used as electrode. Sweep rate = 100 mV/s. The optical bandgap and LUMO level of pristine **ECPblack** were calculated to be 2.7 eV and -2.3 eV, respectively. (See Table S1 for details)

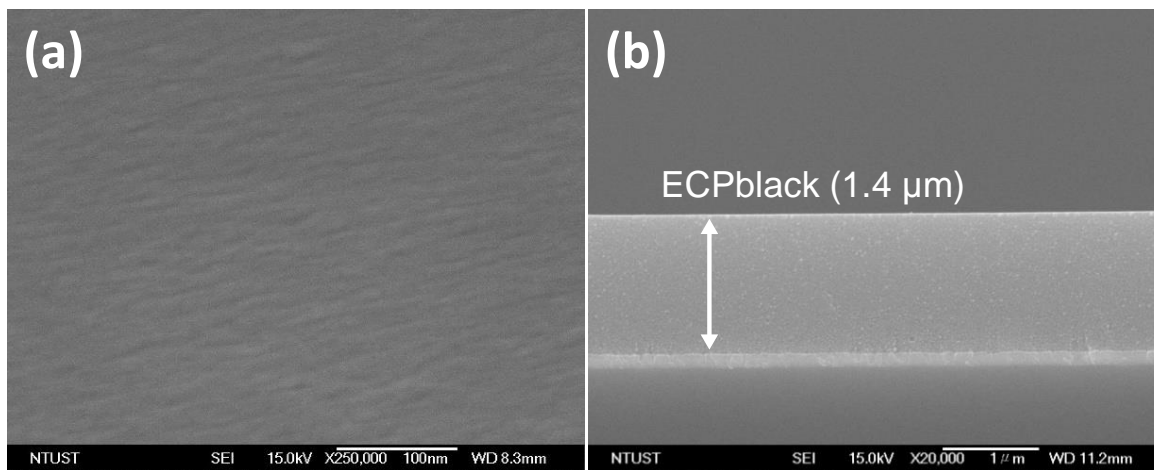


Figure S7. Top-view (a) and cross-sectional (b) SEM images of pristine **ECPblack** on ITO.

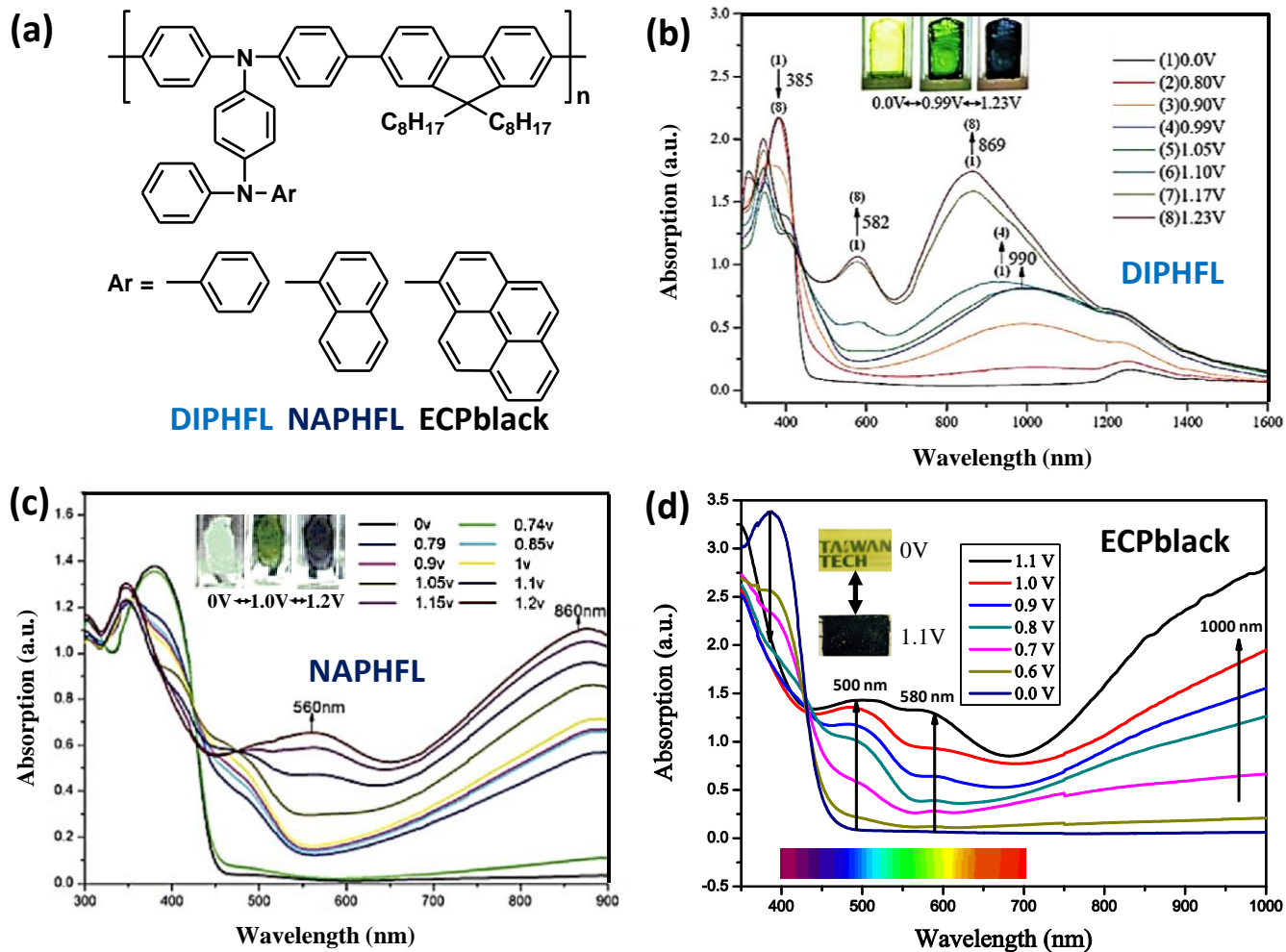


Figure S8. (a) Structures of DIPHFL, NAPHFL and ECPblack. Absorption of (b) DIPHFL, (c) NAPHFL and (d) ECPblack.

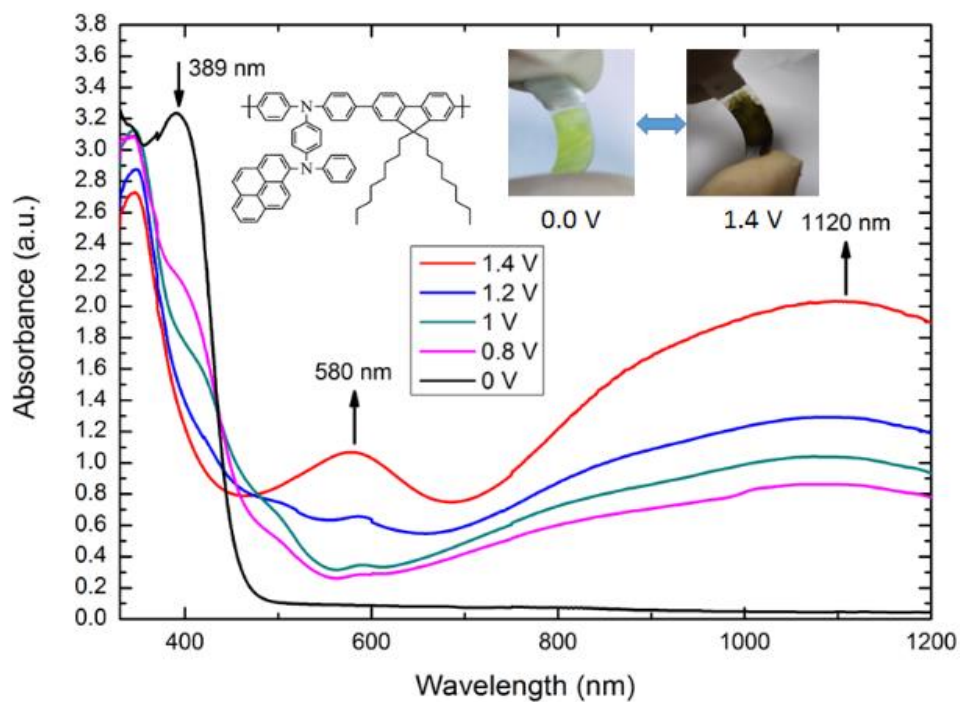


Figure S9. Absorption spectral change of pristine **ECPblack** film on the flexible graphene-PET substrate with increasing of the applied voltage versus Ag/Ag^+ couple as reference. The photo shows the color change of film at indicated applied voltages.

Table S1. Summary of the basic characterizations of ECPblack.

Molecular Weight	Mn × 10⁻⁴ ^a	Mw × 10⁻⁴ ^a	PDI ^a	
ECPblack	2.08	2.93	1.40	
Thermal Properties	T_g (°C) ^b	T_{d10} in N₂ (°C) ^c	T_{d10} in air (°C) ^c	Char yield (%) ^d
ECPblack	169	445	371	62/3
Optical Properties	λ_{max}^{abs} (nm, in toluene) ^e	λ_{max}^{PL} (nm, in toluene) ^e	λ_{max}^{abs} (nm, solid film)	λ_{onset}^{abs} (nm, solid film)
ECPblack	393	514	399	455
Electrochemical Properties	E_g^{opt} (eV) ^f	E_{onset}^{ox} (V) ^g	HOMO (eV) ^h	LUMO (eV) ^h
ECPblack	2.7	0.6	-5.0	-2.3

^a Determined by gel permeation chromatography (GPC) using THF as eluent and polystyrene standards.

^b Glass transition temperatures (T_{gs}) were determined by DSC at a heating rate of 10 °C /min.

^c Decomposition temperatures at 10% weight-loss (T_{d10}) were measured by TGA at a heating rate of 10 °C /min.

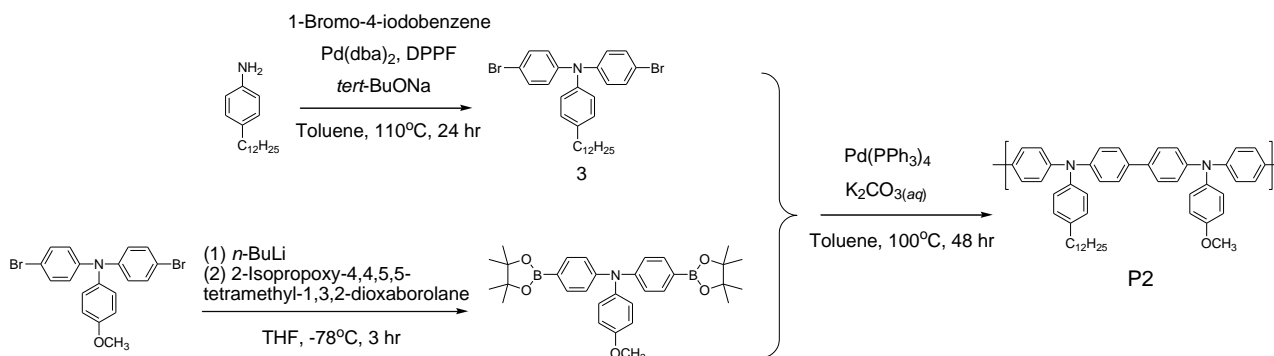
^d Residual weight percentage at 800 °C under nitrogen/air flow.

^e Polymer solution in toluene (ca. 1×10⁻⁵ M solution).

^f Calculated from the UV absorption spectrum of the polymer films by the equation: band gap (eV) = 1240/λ_{onset}^{abs}.

^g The oxidation potential versus Ag/Ag⁺ calculated from CV using ferrocene as an internal standard.

^h Calculated from the equation HOMO = -(E_{onset}^{ox} - E_{onset}^{Fc}) - 4.8 and LUMO = HOMO + band gap.



Scheme S2. Synthetic routes of monomers **3** and polymer **P2**

N,N-bis(4-bromophenyl)-(*p*-methoxy)aniline and *N,N*-bis[4-(4,4,5,5-tetramethyl-1,3,2-dioxaborolan-2-yl)phenyl](*p*-methoxy)aniline were synthesized according to the literatures.⁷

4-Dodecyl-*N,N*-bis(4-bromophenyl) aniline (**3**, Figure S10)

A mixture of 4-dodecylaniline (1 g, 3.8 mmole), 1-bromo-4-iodobenzene (2.7 g, 9.5 mmole), Pd(*dba*)₂ (0.05 g, 0.1 mmole), DPPF (0.1 g, 0.2 mmole) and sodium *tert*-butoxide (1.47 g, 15.3 mmole) in dry toluene (50 ml) was degassed with nitrogen for 30 min while stirring. The mixture was heated and stirred to reflux under nitrogen for 24 hours. After the completion of reaction, 150 ml toluene and 100 ml distilled water were used in extraction. The toluene phase was separated, dried with MgSO₄, filtered and evaporated to dryness. The crude product was purified by silica gel column chromatography using hexane as eluent to give monomer **3** (1.24 g, yield: 57%) as a colorless viscous liquid. ¹H NMR (600 MHz, CDCl₃): δ_H 7.32-7.34 (4H, m, H₁₆), 7.08-7.10 (2H, m, H₁₃), 6.97-7.00 (2H, m, H₁₄), 6.92-6.94 (4H, m, H₁₅), 2.56-2.59 (2H, t, H₁₂), 1.59-1.64 (2H, m, H₁₁) 1.28-1.35 (18H, m, H₂, H₃, H₄, H₅, H₆, H₇, H₈, H₉, H₁₀), 0.89-0.91 (3H, t, H₁); ¹³C NMR (150 MHz, CDCl₃): δ_C 146.7 (C₁₉), 144.4 (C₁₈), 138.9 (C₁₇), 132.2 (C₁₆), 129.5 (C₁₃), 125.0 (C₁₄, C₁₅), 115.0 (C₂₀), 35.4 (C₁₂), 31.9 (C₃), 31.4 (C₁₁), 29.7, 29.7, 29.7, 21.6, 29.5, 29.4, 29.4 (C₄, C₅, C₆, C₇, C₈, C₉, C₁₀), 22.7 (C₂), 14.1 (C₁).

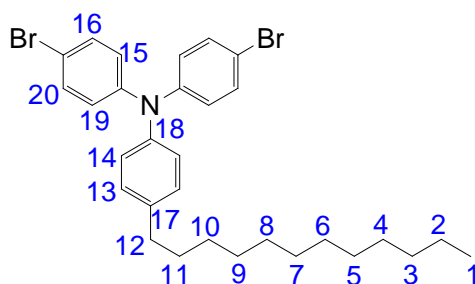


Figure S10. Structure of monomer **3**.

Synthesis of P2 (Figure S11)

In a 50 ml three-necked flask, 401 mg (0.75 mmole) of **3** and 434 mg (0.75 mmole) of *N,N*-bis[4-(4,4,5,5-tetramethyl-1,3,2-dioxaborolan-2-yl)phenyl](*p*-methoxy)aniline were added. The flask was filled with 5 ml of the degassed toluene. Once the two monomers were dissolved, 3 mg Pd(PPh₃)₄ (0.03 mmole) and 10 ml of 2M K₂CO₃ aqueous solution were added, and the mixture was stirred for 48 hours at 100 °C under nitrogen atmosphere. After completion of the reaction, the mixture was cooled to room temperature, and the organic

layer was separated, washed with water and precipitated using methanol. The light celadon fibrous polymer sample was filtered, washed with excess methanol, dried and purified by Soxhlet extraction with acetone for 48 hours to obtain **P2** (0.43 g, yield: 83%) as a green solid. ^1H NMR (600 MHz, CDCl_3): δ_{H} 7.46-7.60 (8H, H_{17} and H_{18}), 7.11-7.16 (14H, H_{14} , H_{16} , H_{19} , H_{20} , H_{21}), 6.89~6.90 (2H, H_{15}), 3.83 (3H, H_1), 2.59~2.61 (2H, H_{13}), 1.64~1.66 (2H, H_{12}), 1.30~1.37 (18H, H_3 , H_4 , H_5 , H_6 , H_7 , H_8 , H_9 , H_{10} , H_{11}), 0.90-0.92 (3H, H_2); ^{13}C NMR (150 MHz, CDCl_3): δ_{C} 156.3 (C_{22}), 146.8, 146.7 (C_{24} and C_{27}), 145.1 (C_{28}), 140.5 (C_{23}), 138.1 (C_{29}), 134.5, 134.1 (C_{25} and C_{26}), 129.2 (C_{21}), 127.4 (C_{14}), 127.2 (C_{17} and C_{18}), 124.9 (C_{20}), 123.8, 123.0 (C_{16} and C_{19}), 114.8 (C_{15}), 55.5 (C_1), 35.4 (C_{13}), 31.9 (C_4), 31.5 (C_{12}), 29.7, 29.6, 29.6, 29.5, 29.4 (C_5 , C_6 , C_7 , C_8 , C_9 , C_{10} , C_{11}), 22.7 (C_3), 14.1 (C_2).

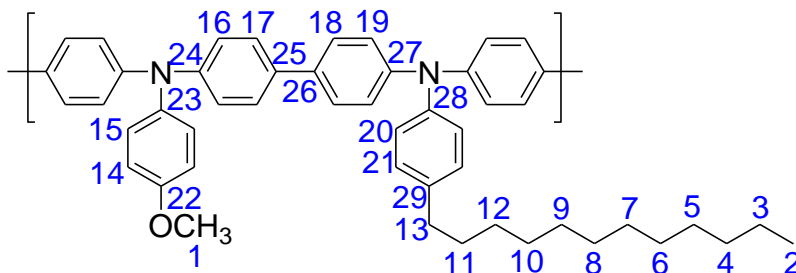


Figure S11. Structure of polymer **P2**.

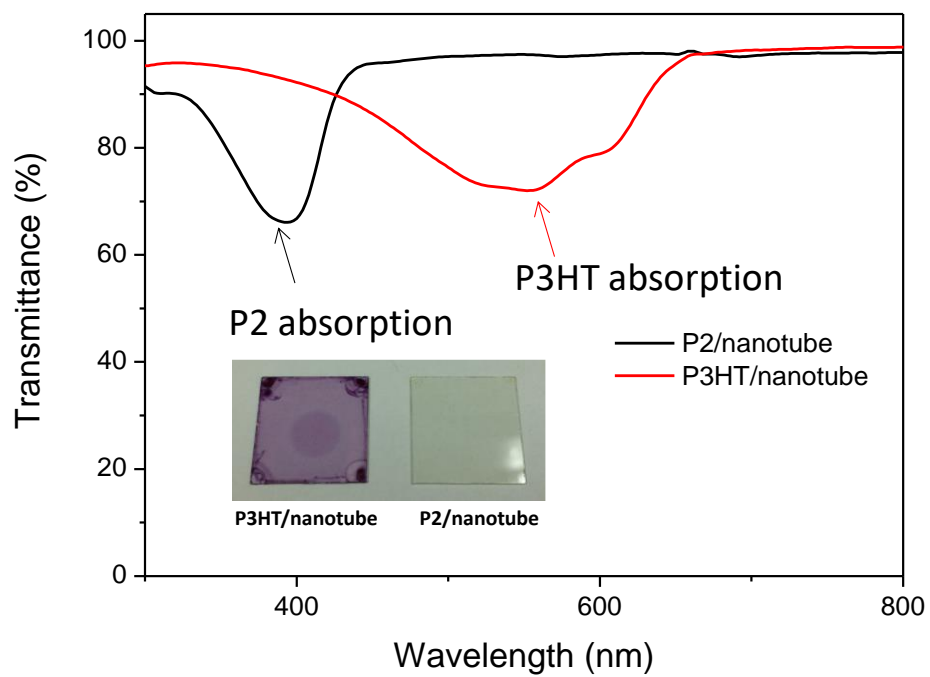


Figure S12. Absorption of **P3HT/SWNT** and **P2/SWNT** films.

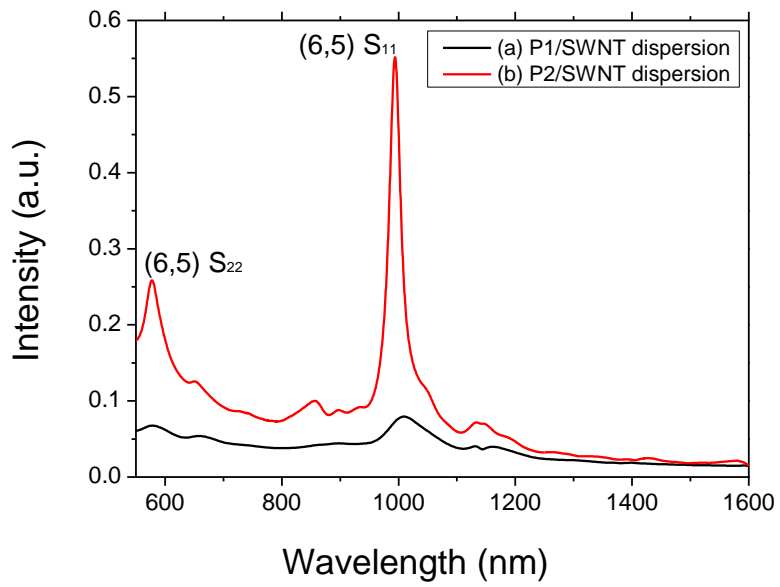


Figure S13. Absorption spectra of (a) **P1/SWNT** and (b) **P2/SWNT** dispersion.

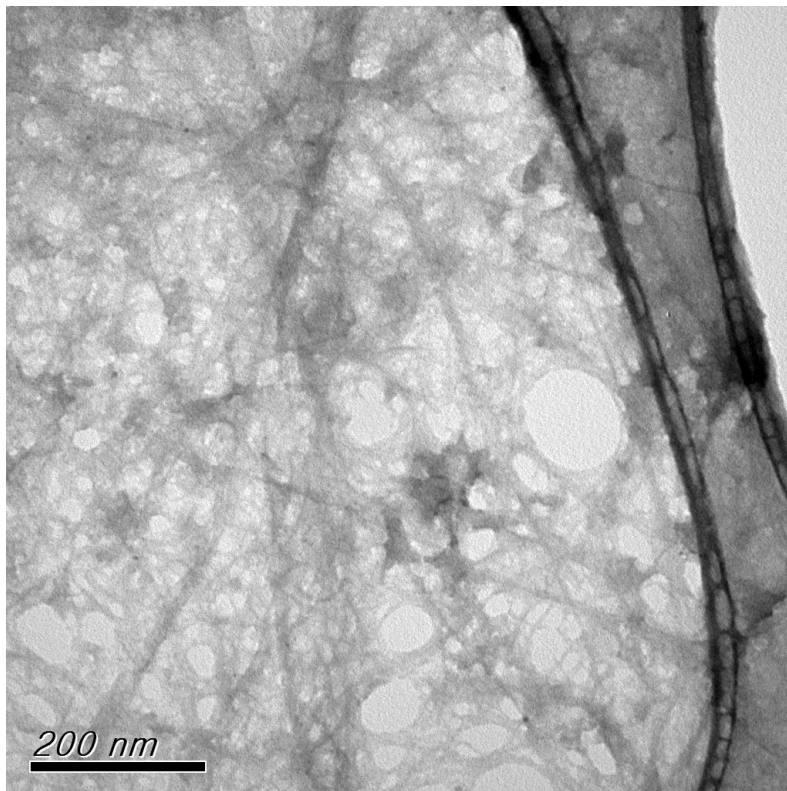


Figure S14. TEM image of SWNT/P2.

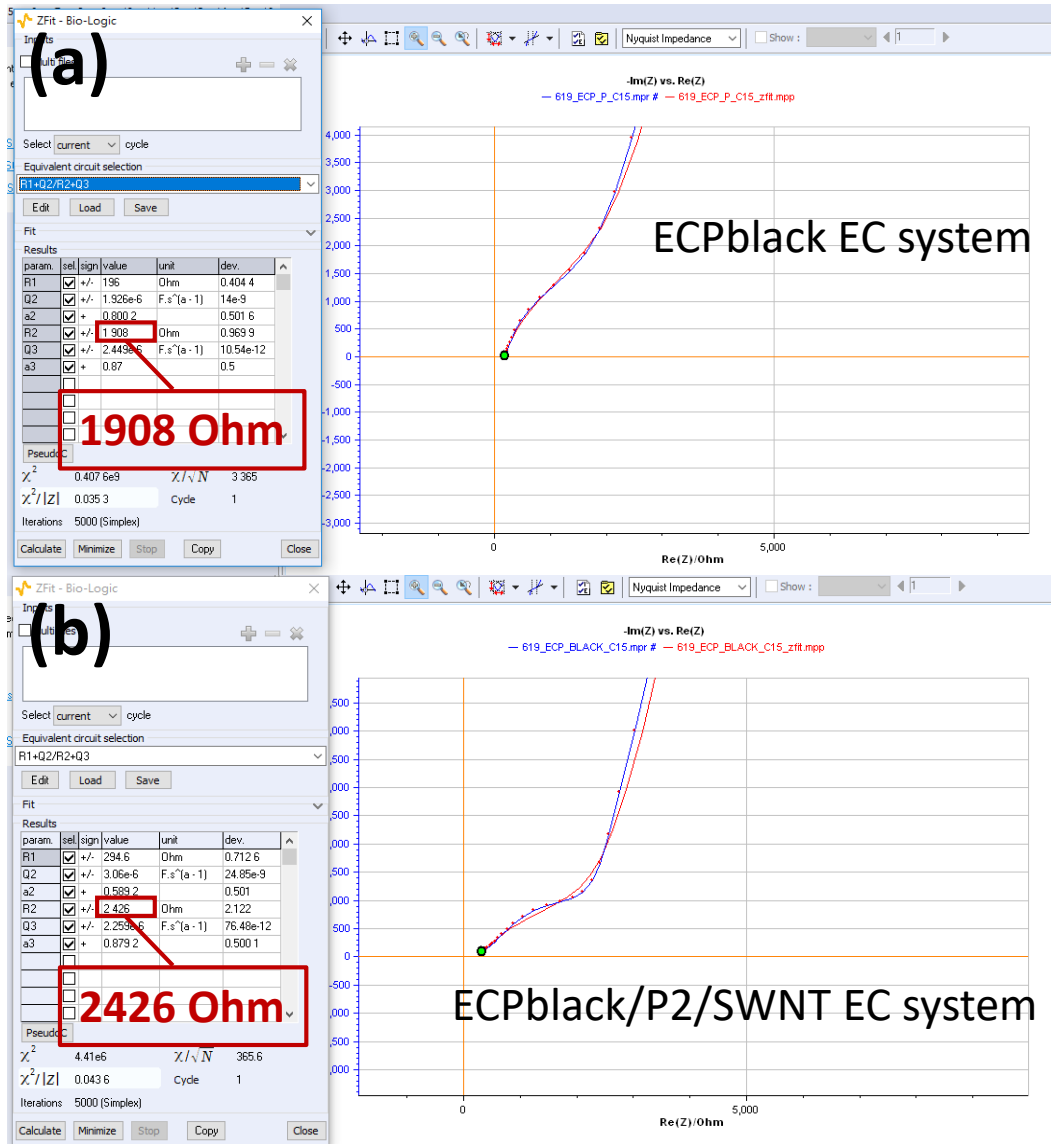


Figure S15. Fitting of (a) ECPblack and (b) ECPblack/P2/SWNT film's impedance behavior.

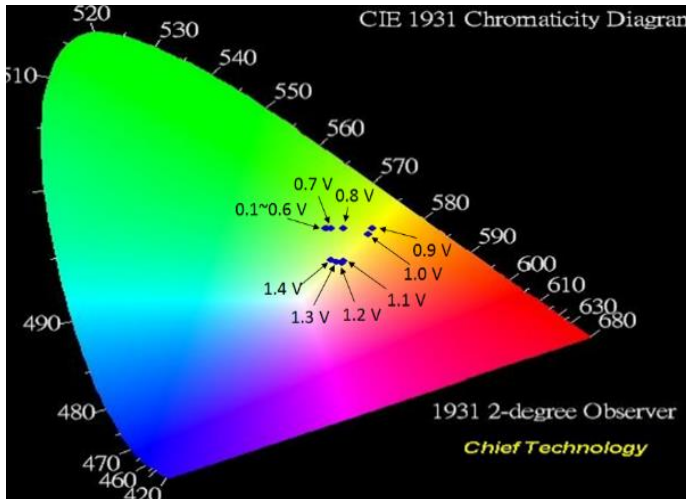
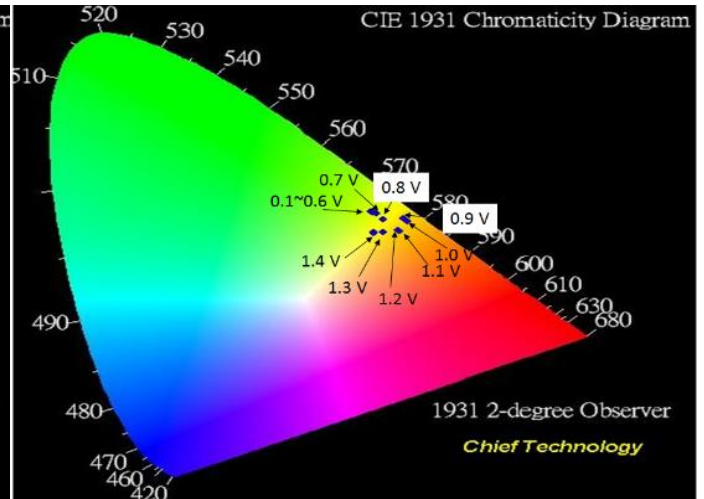
(a)**(b)**

Figure S16. The CIE 1931 UCS (uniform chromaticity scale) diagrams of the luminance under **(a)** 5000 K and **(b)** 3000 K with (u', v') coordinates points.

Under 5000 K			Under 3000 K		
Voltage	u'	v'	Voltage	u'	v'
0.0 V	0.193	0.538	0.0 V	0.218	0.555
0.1 V	0.193	0.538	0.1 V	0.218	0.555
0.2 V	0.193	0.538	0.2 V	0.218	0.555
0.3 V	0.194	0.538	0.3 V	0.218	0.555
0.4 V	0.194	0.538	0.4 V	0.218	0.555
0.5 V	0.194	0.538	0.5 V	0.218	0.555
0.6 V	0.195	0.538	0.6 V	0.222	0.555
0.7 V	0.198	0.539	0.7 V	0.225	0.555
0.8 V	0.207	0.541	0.8 V	0.231	0.554
0.9 V	0.229	0.547	0.9 V	0.246	0.558
1.0 V	0.229	0.542	1.0 V	0.251	0.558
1.1 V	0.228	0.519	1.1 V	0.252	0.550
1.2 V	0.228	0.518	1.2 V	0.240	0.546
1.3 V	0.223	0.518	1.3 V	0.232	0.544
1.4 V	0.217	0.518	1.4 V	0.233	0.543

Theoretical calculation

The theoretical calculations of **ECPblack** were carried out using the Gaussian 09 program package.⁸ We employed the B3LYP exchange correlation functional,^{9,10} combined with the standard double- ζ plus polarization basis set, 6-31G*, to optimize the geometrical molecular structures of Mx, Mx⁺ and Mx²⁺ (Mx means M1, M2 or M3). There was no artificial symmetric or geometric constraint used during the optimization process. HF (Hartree–Fock) was used to calculate the energies and intensities of the 30 lowest-energy electronic transitions of all the Mx species. These were transformed, using the SWizard program,¹¹ into simulated spectra as described before,¹² using Gaussian functions with half-widths of 3000 cm⁻¹, as shown in following Equation:

$$\varepsilon(\omega) = c_1 \sum_I \frac{f_I}{\Delta_{1/2,I}} \exp\left(-2.773 \frac{(\omega - \omega_I)^2}{\Delta_{1/2,I}^2}\right)$$

where ε is the molar extinction coefficient, given in units of M⁻¹·cm⁻¹; the energy ω of all allowed transitions included in the Equation, is expressed in cm⁻¹; f_I and $\Delta_{1/2}$ are representing the oscillator strength and the half-bandwidths (3000 cm⁻¹), respectively.

By using these equations and the model compound, simulation of the oxidation states of **ECPblack** was carried out and the UV-vis spectra of neutral, 1st oxidation and 2nd oxidation states predicted, which are very similar to the experimental results. The difference may arise because the natural difference between the model compound and the polymer.

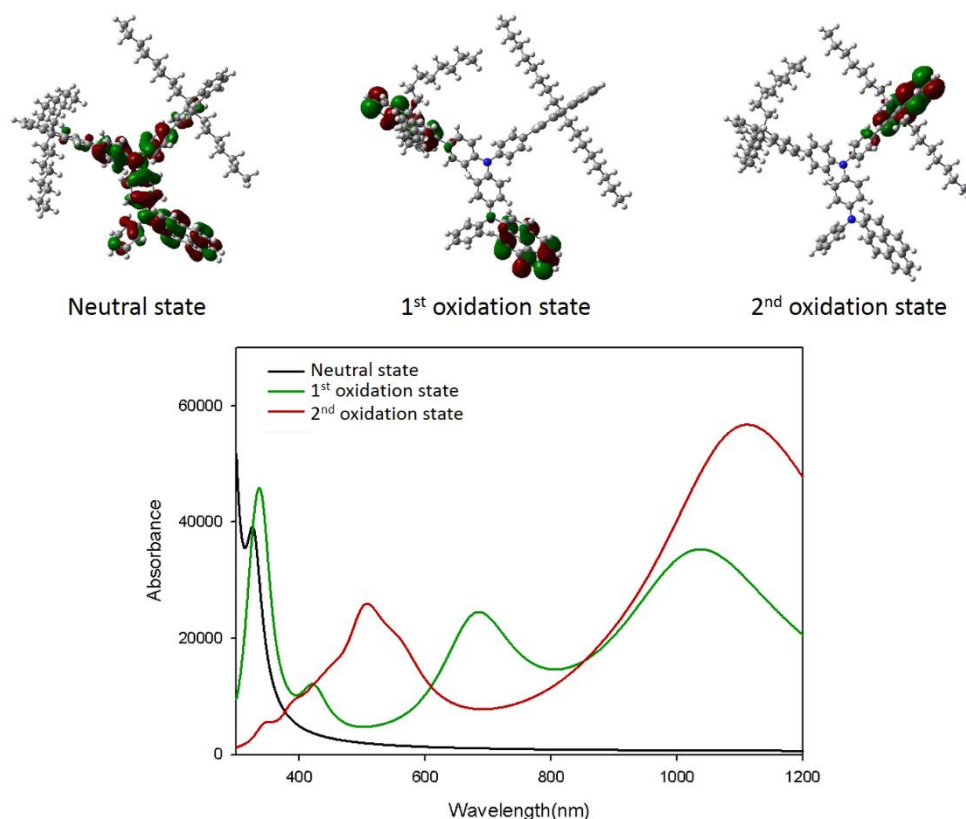


Figure S17. Theoretical calculation of **ECPblack** and oxidized **ECPblack**.

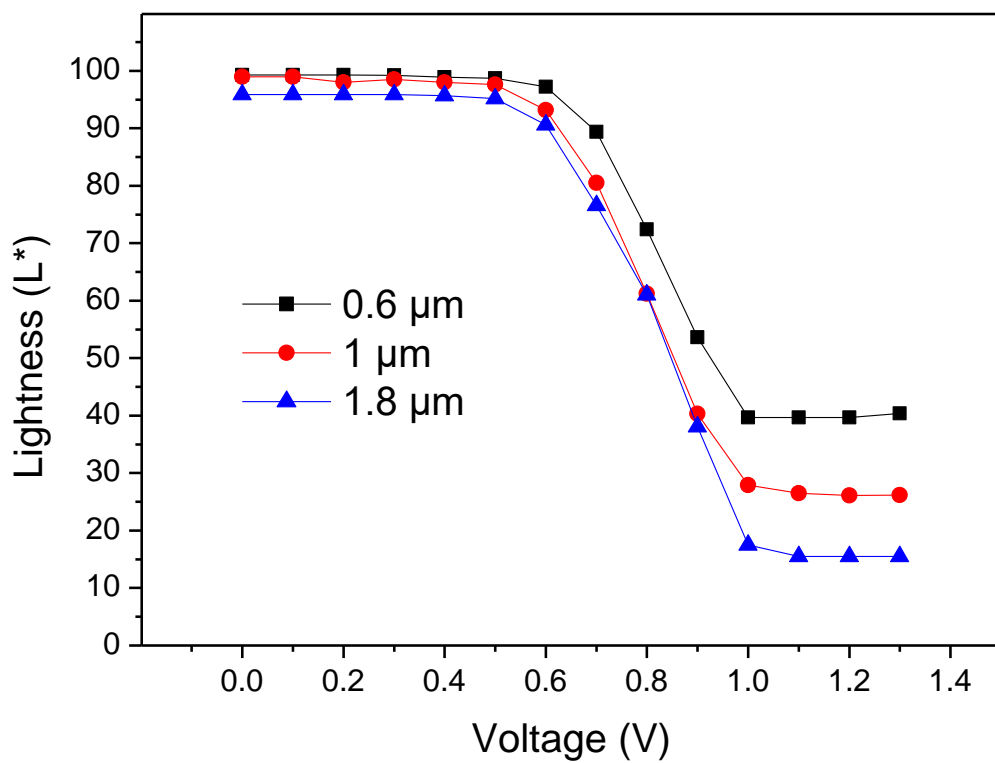


Figure S18. Lightness data of SWNT/P2/ECPblack at a different thickness.

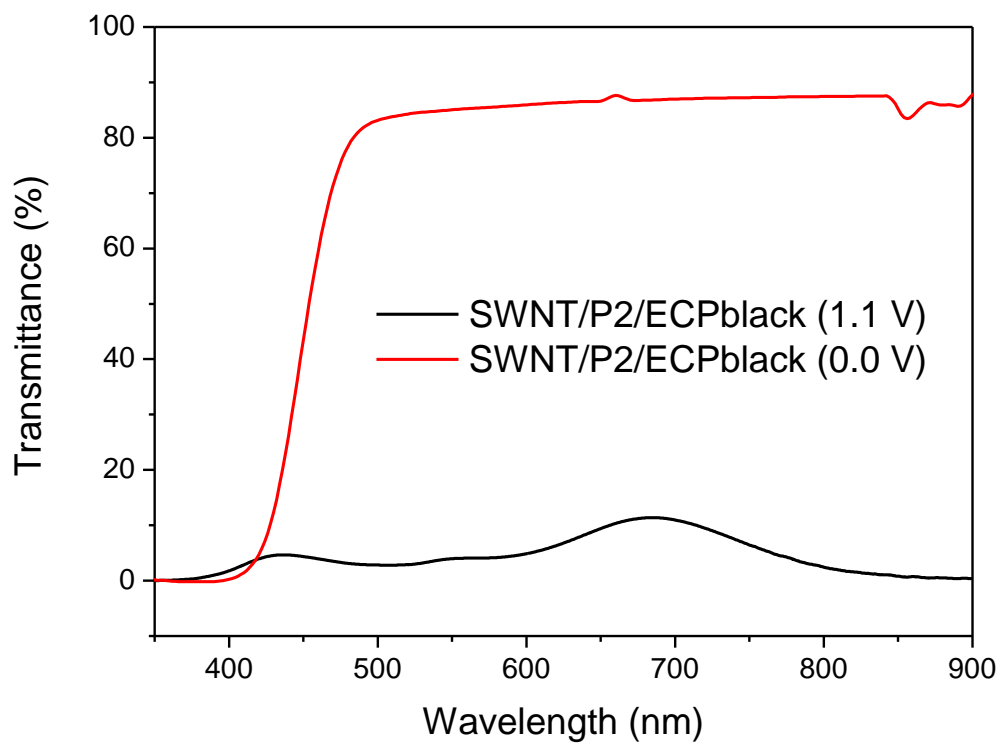


Figure S19. Transmittance of **SWNT/P2/ECPblack** film at a thickness of 1.8 μm.

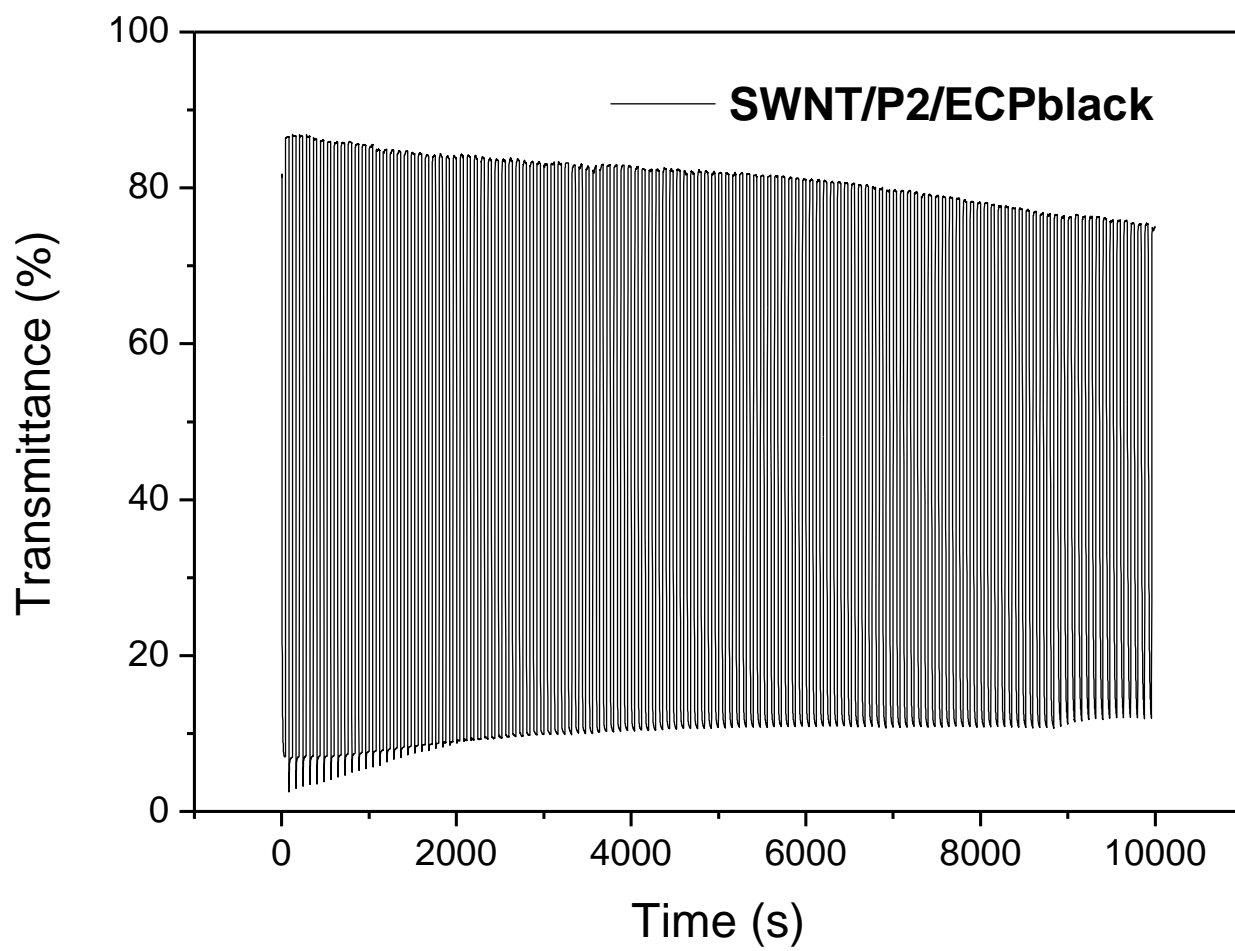


Figure S20. STEP of SWNT/P2/ECPblack.

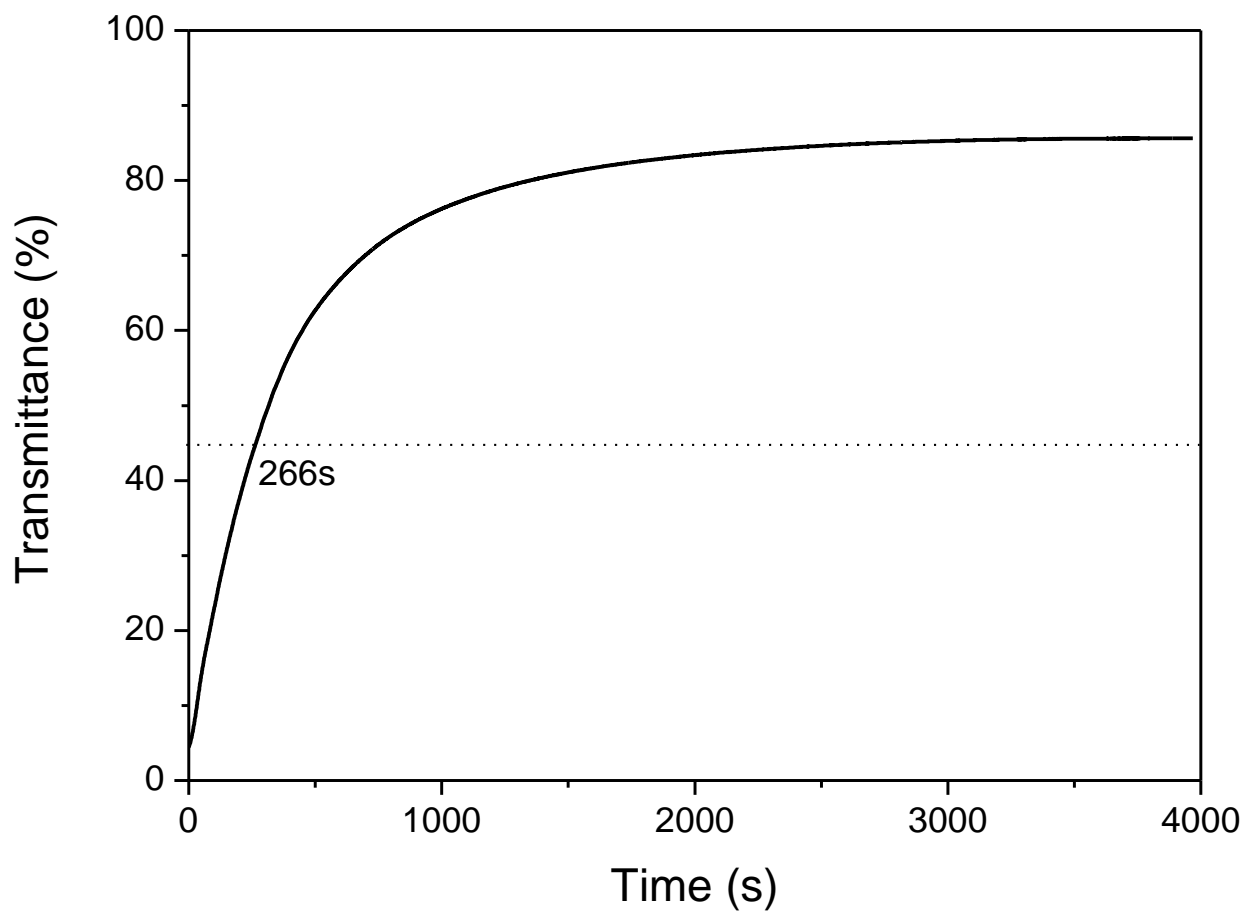


Figure S21. Optical memory property of SWNT/P2/ECPblack film.

Reference:

- S1 D. J. Liaw, P. N. Hsu, W. H. Chen, S. L. Lin, *Macromolecules* **2002**, *35*, 4669-4676.
- S2 W. Li, S. Li, Q. Zhang, S. *Macromolecules* **2007**, *40*, 8205-8211.
- S3 E. Lim, Y. M. Kim, J. I. Lee, B. J. Jung, N. S. Cho, J. Lee, L. M. Do, H. K. Shim, *J. Polym. Sci., Part A: Polym. Chem.* **2006**, *44*, 4709-4721.
- S4 K. R. Justin Thomas, M. Velusamy, J. T. Lin, C. H. Chuen, Y. T. Tao, *J. Mater. Chem.* **2005**, *15*, 4453-4459.
- S5 W. H. Chen, K. L. Wang, W. Y. Hung, J. C. Jiang, D. J. Liaw, K. R. Lee, J. Y. Lai, C. L. Chen, *J. Polym. Sci., Part A: Polym. Chem.* **2010**, *48*, 4654.
- S6 C. Reichardt, *Chem. Rev.* **1994**, *94*, 2319-2358.
- S7 S. F. Völker, T. Dellermann, H. Ceymann, M. Holzapfel, C. Lambert, *J. Polym. Sci. Part A: Polym. Chem.* **2014**, *52*, 890-911.
- S8 M. J. Frisch, G. W. Trucks, H. B. Schlegel, G. E. Scuseria, M. A. Robb, J. R. Cheeseman, G. Scalmani, V. Barone, B. Mennucci, G. A. Petersson, H. Nakatsuji, M. Caricato, X. Li, H. P. Hratchian, A. F. Izmaylov, J. Bloino, G. Zheng, J. L. Sonnenberg, M. Hada, M. Ehara, K. Toyota, R. Fukuda, J. Asegawa, M. Ishida, T. Nakajima, Y. Honda, O. Kitao, H. Nakai, T. Vreven, J. A. Montgomery, J. E. Peralta, F. Ogliaro, M. Bearpark, J. J. Heyd, E. Brothers, K. N. Kudin, V. N. Staroverov, R. Kobayashi, J. Normand, K. Raghavachari, A. Rendell, J. C. Burant, S. S. Iyengar, J. Tomasi, M. Cossi, N. Rega, J. M. Millam, M. Klene, J. E. Knox, J. B. Cross, V. Bakken, C. Adamo, J. Jaramillo, R. Gomperts, R. E. Stratmann, O. Yazyev, A. J. Austin, R. Cammi, C. Pomelli, J. W. Ochterski, Martin, R. L. K. Morokuma, V. G. Zakrzewski, G. A. Voth, P. Salvador, J. J. Dannenberg, S. Dapprich, A. D. Daniels, Ö. Farkas, J. B. Foresman, J. V. Ortiz, J. Cioslowski, D. J. Fox, Vol. Gaussian 09, Revision A.1. , Gaussian, Inc., Wallingford CT, **2009**.
- S9 A. D. Becke, *J. Chem. Phys.* **1993**, *98*, 5648-5652.
- S10 C. Lee, W. Yang, R. G. Parr, *Physical Review B* **1988**, *37*, 785-789.
- S11 S. I. Gorelsky, AOMix: Program for Molecular Orbital Analysis, York University: Toronto, **1997**.
- S12 S. I. Gorelsky, *Comprehensive Coordination Chemistry II*, Elsevier Pergamon: New York, **2003**.